The precision of gingival recession measurements is increased by an automated curvature analysis method

Marko Kuralt (marko.kuralt@kclj.si)
University Medical Centre Ljubljana
Rok Gašperšič
University Medical Centre Ljubljana
Aleš Fidler
University Medical Centre Ljubljana

Research Article

Keywords: gingival recession, curvature, digital measurement, cemento-enamel junction, precision

Posted Date: September 7th, 2021

DOI: https://doi.org/10.21203/rs.3.rs-745256/v1

Abstract

Background

The extent of gingival recession represents one of the most important measures determining outcome of periodontal plastic surgery. The accurate measurements are, thus, critical for optimal treatment planning and outcome evaluation. Present study aimed to introduce automated curvature-based digital gingival recession measurements, evaluate the agreement and reliability of manual measurements, and identify sources of manual variability.

Methods

Measurement of gingival recessions was performed manually by three examiners and automatically using curvature analysis on representative cross-sections (n = 60). Cemento-enamel junction (CEJ) and gingival margin (GM) measurement points selection was the only variable. Agreement and reliability of measurements were analysed using intra- and inter-examiner correlations and Bland-Altman plots. Measurement point selection variability was evaluated with manual point distance deviation from an automatic point. The effect of curvature on manual point selection was evaluated with scatter plots.

Results

Bland-Altman plots revealed a high variability of examiner's recession measurements indicated by high 95% limits of agreement range of approximately 1mm and several outliers beyond the limits of agreement. CEJ point selection was the main source of examiner's variability due to smaller curvature values than GM, i.e., median values of -0.98mm^{-1} and − 4.39mm^{-1}, respectively, indicating straighter profile for CEJ point. Scatter plots revealed inverse relationship between curvature and examiner deviation for CEJ point, indicating a threshold curvature value around 1mm^{-1}.

Conclusions

Automated curvature-based approach increases the precision of recession measurements by reproducible measurement point selection. Proposed approach allows evaluation of teeth with indistinguishable CEJ that could be not be included in the previous studies.

1. Background

The extent of gingival recession, i.e., recession depth, is evaluated before and after treatment and represents one of the most important measures determining treatment outcome [1]. Recession depth is a measure used to quantify treatment success in terms of percentage of root coverage and defects with

complete root coverage, enabling comparison between different treatment techniques [1, 2]. Therefore, the accuracy of recession depth measurements is critical for diagnosis, optimal treatment planning, and outcome evaluation.

The standard method for gingival recession evaluation is an assessment with the periodontal probe, allowing precise evaluation at a clinically acceptable level [3, 4]. However, the following limitations should be considered, i.e., variations in position and angulation of the periodontal probe and rounding errors [5–7]. Rounding errors were eliminated with utilization of digital callipers with resolution of 0.01 mm either with pair of dividers [8] or endodontic spreader [9]. While, 3D digital measuring method [10, 11] eliminated both limitations. In brief, the measurement site and direction were defined by selecting a cross-section aligned with the tooth's long axis, eliminating the variations in position and angulation of the periodontal probe. At the same time, utilisation of a digital ruler allowing for measurements to the nearest 0.01 mm increased the measurement's accuracy and eliminated rounding of measurements to the nearest mm as with a periodontal probe.

By definition, recession depth is defined as a distance between anatomical landmark, i.e., the cemento-enamel junction (CEJ), and gingival margin (GM) [12]. Thus, the accuracy of recession depth measurements strongly depends on the measurement point selection. The precise determination of the CEJ was already outlined as a significant limitation, reducing the reliability and reproducibility of recession depth measurements [13, 14]. Furthermore, precise localisation of CEJ is hampered by poor visibility, carious or non-carious cervical lesions or cervical restorations [15, 16]. Pini-Prato et al. [17] showed that almost 40% of teeth with gingival recession exhibit unidentifiable CEJ, rendering repeated measurements using the CEJ nearly impossible and prone to errors during follow-up.

By definition, from medical image analysis, landmarks are well-defined points that can be identified based on distinguishable shape features and can be placed manually by examiners or detected automatically [18, 19]. With recent advancements, automated image analysis based on geometric properties is gaining increased importance in dentistry [20–24]. One of the widely used geometric properties is curvature [25, 26], a mathematical measure describing a deviation of a curve from being a straight line. In dentistry, curvature analysis was already applied for facial profile landmarking in orthodontics [27] and teeth dimension measurements [28], exhibiting reliable and reproducible evaluation. Up to now, the curvature analysis has not been used in the evaluation of gingival recessions.

The present study aimed to 1) introduce automated digital measurements of recession depth by using curvature analysis, 2) evaluate the agreement and reliability of manual digital measurements with examiners with different level of experience, 3) identify the sources of examiner's variability by using curvature analysis, and 4) evaluate the agreement of automated digital and clinical measurements.

2. Methods

2.1 Sample

An existing dataset of digital dental models of patients presenting with gingival recessions referred to the Department of Oral Medicine and Periodontology, University Medical Centre Ljubljana, Slovenia, was used to compare digital measurements of gingival recessions. The digital dental models were acquired by intraoral scanning (CEREC Omnicam AC, Dentsply Sirona; software version: SW 4.5.2) when the first author, i.e., experienced operator, was present at the Department in the year 2019. Thus, the dataset is representing a convenience sample. The National Medical Ethics Committee approved the study (Protocol No. 0120–595/2018/4), and the study was conducted in accordance with the Helsinki Declaration as revised in 2013.

The complete dataset was screened for study eligibility by the first author prior to study entry. Digital dental models were eligible for inclusion when gingival recession defect was present at any tooth either in the upper or lower arch and only when the affected teeth presented with identifiable natural CEJ, i.e., Class A- and A + in the Classification of root surface concavities by [17]. In cases where multiple digital dental models from the same patient were available, e.g., follow-up models after root coverage, only the baseline model was used. In patients presented with multiple gingival recessions, each gingival recession defect was referred to as an individual unit.

The study sample consisted of digital dental models obtained from ten patients, resulting in 52 teeth with gingival recession with identifiable natural CEJ. Due to the inclusion of molars with the gingival recession at both roots at the buccal side, 60 measuring sites were collected. The distribution of measuring sites per tooth group were: 10 incisors (7 maxillary and 3 mandibular), 10 canines (9 maxillary and 1 lower), 20 premolars (18 maxillary and 2 lowers), and 20 molars (all maxillary).

2.2 Comparison of digital measurements of recession depth

Included digital dental models were then imported into the 3D data measurement analysis software (GOM Inspect 2017; GOM GmbH). A local coordinate system was created for each tooth of interest, with a long axis of the tooth matching the *z*-axis and mesio-distal direction matching the *x*-axis. Digital dental models were refined with "Refine mesh" tool (with "Minimal edge length" setting set at 0.01 mm) to enhance the digital model quality and resolution. A representative bucco-oral cross-section was then manually selected at the central buccal site in the direction of the tooth's long axis. In molars, a bucco-oral cross-section was created for each root if the gingival recession was present at the corresponding root.

Measurements of gingival recessions were performed independently by manual and automatic approach. In the cross-section images, two measurement points, representing CEJ and GM, were determined manually and automatically, followed by an automated distance measurement.

For the manual method, three examiners with different digital analysis experience performed the measurement point selection on the cross-sections (Fig. 1a-c). Examiner No. 2 is the only examiner experienced in digital analysis. Additionally, Examiner No. 3 is experienced in clinical diagnostics, i.e., a

standard calibrated examiner for clinical periodontal measurements. The process of measurement point selection was repeated one week later by all three examiners. The order of cross-sections was randomised for each examiner, reducing the possible bias in the repeated measurements.

For the automatic method, the shape of each cross-section was mathematically described by the curvature. Curvature was computed by the software's "Compute Curve Curvature" tool describing a cross-section curve with a mathematical function, i.e., spline function. From this spline curve, curvature values were determined for each point at a distance of 0.01 mm. Obtained curvature values were then visualised with colour-coded "curvature combs" [29], i.e., graphs that display the amount of curvature at a specific point on the cross-section (Fig. 1d).

Based on the obtained curvature values, two cross-section segments of interest were recognised on all cross-sections, i.e., CEJ and GM. CEJ segment is represented by the transition from convex to concave shape in corono-apical direction. In contrast, the GM segment is represented by the transition from convex to concave shape in the opposite direction, i.e., apico-coronal. For precise measurement point selection, local extreme curvature values in the concave part of both segments mentioned above were determined as CEJ and GM points (Fig. 1d). GM point was determined based on the established gingival margin definition [30]. CEJ point decision was based on existing literature [28, 31–33]. After the determination of points of interest, points are then selected automatically.

After either manual or automatic measurement point selection, a gingival recession was measured automatically as a distance between the measurement points.

2.3 Evaluation of manual measurement point selection variability

Measurement point selection variability was measured as a distance of manual measurement point in reference to automated curvature-based point position on a cross-section. The distance was obtained with the software's "Arc length" tool. It was performed for both the CEJ and GM measurement points. Results were presented using box-plots with positive values representing coronal deviation and negative values apical deviation of manual measurement points.

Furthermore, for CEJ measurement point, the effect of curvature on manual point selection deviation was evaluated by creating curvature vs examiner deviation scatter plots.

2.4 Comparison of digital and clinical recession depth measurements

Obtained automated digital measurements were compared to clinical measurements of recession depth. Clinical measurements were collected retrospectively from patient's records and were performed by Examiner No. 3.

2.5 Statistical analysis

Statistical analysis was carried out using a statistical software program (IBM SPSS Statistics version 25; IBM Corp). Descriptive statistics, including mean, standard deviations, median, minimum, and maximum values, were obtained.

For evaluation of the examiners' bias, i.e., reliability or inter-examiner variability, and ability of the examiners to repeat multiple measurements, i.e., reproducibility or intra-examiner variability, the intraclass correlation coefficient (ICC) and confidence intervals were calculated.

Agreement of the digital measurements between examiners was analysed using Bland-Altman plots using the curvature-based approach as a reference. The mean differences between tested groups were assessed using the one-sample t-test to determine if mean differences were statistically different from zero.

Agreement of the automated digital and clinical approach was analysed using Bland-Altman plot using the automated curvature-based approach as a reference.

3 Results

3.1 Recession depth measurements

Median recession depth obtained with an automated curvature-based approach for a study sample (n = 60) was 1.90 mm (25th – 75th percentile: 1.25–2.62 mm), representing a sample of predominately shallow gingival defects.

3.2 Agreement and reliability of digital recession depth measurements

Based on the inter- and intra-examiner reliability with high lower boundary values of the 95% confidence intervals, i.e., 0.93 and 0.94, respectively, the manual approach can be considered excellent regarding precision.

The mean differences between the manual and automated approach on Bland-Altman plots were around zero (Fig. 2). A statistically significant difference was found only for Examiner No.1 in the first round of measurements compared to the automated measurements ($p < 0.001$) (Fig. 2a). The high variability of recession depth measurements was found for all three examiners, indicated by high 95% limits of agreement range of approximately 1 mm and outliers beyond the limits of agreement (Fig. 2).

3.3 Manual measurement point selection deviation

A small median difference was found for both CEJ and GM points, except for Examiner No. 1's first-round (Fig. 3). High variability was found for CEJ compared to the GM point, indicated by a high interquartile range and several outliers (Fig. 3a).

The shape description of CEJ and GM profiles using curvature showed that CEJ's profiles are straighter than GM profiles, with a median value closer to zero (Fig. 4). Box-plots also revealed that CEJ profiles exhibit a smaller range than GM profiles (Fig. 4), despite visually more considerable shape differences between CEJ profiles, as depicted by visual inspection of cross-sections (Fig. 5).

The scatter plots revealed inverse relationship between curvature and examiner deviation distance for CEJ point, indicating a threshold curvature value around 1 mm^{-1} (Fig. 6), with the exception of Examiner No. 1's first round of measurements (Fig. 6a). Below this threshold value, the variability of deviation increase.

3.4 Agreement of digital and clinical recession depth measurements

The mean difference between the automated digital and clinical approach was − 0.52 mm as depicted by Bland-Altman plot (Fig. 7). The high variability of recession depth measurements was found for the clinical approach, indicated by high 95% limits of agreement range of approximately 2.7 mm (Fig. 7).

4. Discussion

Accurate evaluation of gingival recession dimensions is an essential part of the diagnosis, treatment planning, and outcome evaluation. In the present study, curvature analysis was used to accurately automate the measurement point selection required for recession depth measurement and analyse the examiners' measurement error. The main source of variability for examiners was CEJ measurement point selection. The automated measurements of recession depth using curvature analysis reduce human variability and increase the precision of measurements.

In the present study, a sample of predominately shallow gingival defects was used to compare approaches due to the inclusion of teeth with identifiable natural CEJ only. Shallow gingival defects presenting with small recession depths are hard to evaluate with a periodontal probe due to mentioned limitations of measurement accuracy [5–7]. However, as already outlined by [10], increased resolution of digital measurements to the nearest 0.01 mm enables evaluation of shallow gingival defects as well. Additionally, the importance of measurement accuracy was also emphasised with a superb illustration of the effect of rounding digital measurements on two important parameters for evaluating the success of different treatment techniques, i.e., percentage of root coverage [34] and percentage of defects with complete root coverage [10, 34].

Manual digital measurements of gingival recession exhibit high variability depicted by Bland-Altman plots. Errors are an inherent part of manual measurements and are unavoidable with human involvement [35]. Therefore, for objective comparison of variability between examiners and the unknown true value of recession depth, an automated curvature-based approach was used as a reference method due to automaticity enabling perfect reproducibility of repeated measurements. Despite excellent ICC values and

non-significant mean differences between the approaches, Bland-Altman plots revealed a relatively high variability of recession depth measurements with a 95% limit of agreements range of approximately 1 mm. Despite inexperience in digital analysis, Examiner No. 3, being experienced in clinical diagnostics, exhibited the smallest range of 95% limits of agreement, i.e., 0.57 mm. Obtained variability range is much smaller than evaluation with a periodontal probe, i.e., around 2.5 mm, and similar to evaluation with a digital manual approach, i.e., around 1 mm, supported by our results (Fig. 7) and also found in other studies [3, 4]. In contrast to previous digital studies, the only variable part in the present study was measurement point selection; thus, obtained variability can be attributed solely to the measurement points selection. The digital manual approach utilised in the previous studies [3, 4] measured gingival recessions on the digital models and not on cross-sections, including measuring direction and angle variability, into the comparison. The implementation of the proposed approach is straightforward. It requires only a single 3D data measurement analysis software that is free for non-commercial use.

Importantly, the main source of variability is the CEJ measurement point. Both the manual and the automated approach used the shape of the cross-section for the measurement point selection. The main difference between the approaches was the examiners' subjective bias. Our results revealed that the main variability could be attributed to the position of the CEJ measurement point (Fig. 3a), despite inclusion criteria with visible and identifiable CEJ. Curvature analysis revealed a straighter CEJ profile compared to the GM profile, outlined with smaller absolute curvature values (Fig. 4), resulting in a less distinct shape feature than the gingival margin (Fig. 5). Our findings were supported by scatter plots revealing that absolute curvature values of approximately 1 mm^{-1} represent an arbitrary threshold where higher deviations in measurement point position can be observed (Fig. 6). To outline the magnitude of the problem, half of the cases exhibit CEJ with curvature less than 1 mm^{-1}. Furthermore, a great example is comparing the first and second round of measurements for Examiner No. 1 with larger deviations present at higher absolute curvature values as well in the first round. In contrast, in the second round, a "learning effect" was observed with improving precision over the higher range, but importantly, not below the mentioned threshold.

This study was subject to some limitations. First, either measurement point's true position is impossible to determine; therefore, the trueness of measurements could not be evaluated. Despite the perfect reproducibility of point selection presented automated approach requires initial human input to determine the points of interest. In the present study, the point definition was based on definitions from existing literature. However, with time, both the cement and enamel wears away due to the exposure of tooth's root surface to the oral environment [17], rendering CEJ a questionable landmark. The automated curvature-based approach is applicable beyond the limitations of identifiable CEJ, meaning that when defects or restorations are present, the edges of the defect or restorations can be objectively defined by curvature analysis as well. Thus, in digital analysis, the term and landmark of CEJ might have been redefined to "coronal reference point" in the scope of the periodontal measurements. Additionally, curvature analysis can also aid in describing root surface defects' morphology, opening novel insights into the

reconstruction of anatomical CEJ before root coverage [36, 37]. However, further research is required for validation in cases without identifiable natural CEJ.

Second, compared to a whole 3D model, a cross-section represents only one out of many available measuring sites. Further research is required to explore novel possibilities analysing whole 3D models. Nonetheless, cross-sections are widely used to evaluate tissue dynamics in periodontal plastic surgery [34, 38–42] and implantology [43–45], enabling great standardisation regarding the selection of measuring site and direction of measurement. Measurement site selection, e.g., selecting a representative cross-section, is also one of the possible variabilities in the measurement of recession depth. For follow-up measurements measuring site variability was eliminated with superimposition of digital models [11, 39], also stating the importance of superimposition accuracy [46].

Third, while the clinical approach utilizes also the colour properties as the additional visual reference, only shape properties were used in the present study. Despite color acquisition of digital dental models in the study, export of color models for further analysis was unavailable due to software limitations. Exporting of color models has become available only recently for some systems and color models proved to be useful in digital measurements of keratinized tissue width with main emphasis on color difference [47]. Further research could be aimed to test the suitability of colour properties on automated CEJ detection.

5. Conclusion

Novel automated approach increases the precision of gingival recession measurements by using curvature analysis, opening novel possibilities for comparison of different treatment techniques. The utilisation of curvature analysis enables completely reproducible measurement point selection, eliminating human variability and allowing the evaluation of teeth with indistinguishable CEJ that were often excluded in the previous studies. Therefore, future studies could be done on larger, more clinically relevant samples.

Abbreviations

3D
Three-dimensional
CEJ
Cemento-enamel junction
GM
Gingival margin
ICC
Intraclass correlation coefficient

Declarations

Ethics approval and consent to participate: The National Medical Ethics Committee approved the study (Protocol No. 0120-595/2018/4), and the study was conducted in accordance with the Helsinki Declaration as revised in 2013.

Consent for publication: Not applicable.

Availability of data and materials: The data supporting the study's findings are available in this article's supplementary material. Additionally, digital models used in the present study will be openly available as supplementary material.

Competing interests: The authors declare that they have no competing interests.

Funding: The study was supported by the Ministry of Higher Education, Science, and Technology, Republic of Slovenia, under grant number P3-0293. The funding body did not involve in the study design, data collection, data analysis, interpretation of data and writing the manuscript.

Authors' contributions: M.K. contributed to conception and design of the study and article, acquired the digital model dataset, performed the analysis, interpret the data, drafted the article, and prepared figures; R.G. acquired the clinical measurements dataset, performed the analysis, interpret the data, and revised the article; A.F. contributed to conception and design of the study and article, performed the analysis, interpret the data, and revised the article. All authors have read and approved the manuscript.

Acknowledgements: Not applicable.

References

1. P. Cortellini, N.F. Bissada, Mucogingival conditions in the natural dentition: Narrative review, case definitions, and diagnostic considerations, J. Clin. Periodontol. 45 (2018) S190–S198. https://doi.org/10.1111/jcpe.12948.
2. G. Pini-Prato, C. Magnani, F. Zaheer, J. Buti, R. Rotundo, Critical Evaluation of Complete Root Coverage as a Successful Endpoint of Treatment for Gingival Recessions, Int. J. Periodontics Restorative Dent. (2017). https://doi.org/10.11607/prd.2400.
3. D. Schneider, A. Ender, T. Truninger, C. Leutert, P. Sahrmann, M. Roos, P. Schmidlin, Comparison between clinical and digital soft tissue measurements, J. Esthet. Restor. Dent. 26 (2014) 191–199. https://doi.org/10.1111/jerd.12084.
4. H.N. Fageeh, A.A. Meshni, H.A. Jamal, R.S. Preethanath, E. Helboub, The accuracy and reliability of digital measurements of gingival recession versus conventional methods, BMC Oral Health. 19 (2019) 1–8. https://doi.org/10.1186/s12903-019-0851-0.
5. A.F. Hefti, Periodontal probing, Crit. Rev. Oral Biol. Med. 8 (1997) 336–356. https://doi.org/10.1177/10454411970080030601.

6. S.G. Grossi, R.G. Dunford, A. Ho, G. Koch, E.E. Machtei, R.J. Genco, Sources of error for periodontal probing measurements, J. Periodontal Res. 31 (1996) 330–336. https://doi.org/10.1111/j.1600-0765.1996.tb00500.x.
7. T.L.P. Watts, Probing site configuration in patients with untreated periodontitis: A study of horizontal positional error, J. Clin. Periodontol. (1989). https://doi.org/10.1111/j.1600-051X.1989.tb02331.x.
8. M.P. Santamaria, F.F. Suaid, M.Z. Casati, F.H. Nociti, A.W. Sallum, E.A. Sallum, Coronally Positioned Flap Plus Resin-Modified Glass Ionomer Restoration for the Treatment of Gingival Recession Associated With Non-Carious Cervical Lesions: A Randomized Controlled Clinical Trial, J. Periodontol. 79 (2008) 621–628. https://doi.org/10.1902/jop.2008.070285.
9. S. Bittencourt, É. Del Peloso Ribeiro, E.A. Sallum, A.W. Sallum, F.H. Nociti, M.Z. Casati, Comparative 6-Month Clinical Study of a Semilunar Coronally Positioned Flap and Subepithelial Connective Tissue Graft for the Treatment of Gingival Recession, J. Periodontol. 77 (2006) 174–181. https://doi.org/10.1902/jop.2006.050114.
10. O. Zuhr, S.F. Rebele, D. Schneider, R.E. Jung, M.B. Hürzeler, Tunnel technique with connective tissue graft versus coronally advanced flap with enamel matrix derivative for root coverage: A RCT using 3D digital measuring methods. Part I. Clinical and patient-centred outcomes, J. Clin. Periodontol. 41 (2014) 582–592. https://doi.org/10.1111/jcpe.12178.
11. S.F. Rebele, O. Zuhr, D. Schneider, R.E. Jung, M.B. Hürzeler, Tunnel technique with connective tissue graft versus coronally advanced flap with enamel matrix derivative for root coverage: A RCT using 3D digital measuring methods. Part II. Volumetric studies on healing dynamics and gingival dimensions, J. Clin. Periodontol. 41 (2014) 593–603. https://doi.org/10.1111/jcpe.12254.
12. G. Pini Prato, Mucogingival deformities., in: Ann. Periodontol., 1999: pp. 98–101. https://doi.org/10.1902/annals.1999.4.1.98.
13. G. Zucchelli, T. Testori, M. De Sanctis, Clinical and Anatomical Factors Limiting Treatment Outcomes of Gingival Recession: A New Method to Predetermine the Line of Root Coverage, J. Periodontol. 77 (2006) 714–721. https://doi.org/10.1902/jop.2006.050038.
14. H.U. Hug, M.A. Van 't Hof, A.J. Spanauf, H.H. Renggli, Validity of Clinical Assessments Related to the Cemento-enamel Junction, J. Dent. Res. 62 (1983) 825–829. https://doi.org/10.1177/00220345830620071301.
15. P.A. Heasman, M. Ritchie, A. Asuni, E. Gavillet, J.L. Simonsen, B. Nyvad, Gingival recession and root caries in the ageing population: a critical evaluation of treatments, J. Clin. Periodontol. (2017). https://doi.org/10.1111/jcpe.12676.
16. P.A. Heasman, R. Holliday, A. Bryant, P.M. Preshaw, Evidence for the occurrence of gingival recession and non-carious cervical lesions as a consequence of traumatic toothbrushing, J. Clin. Periodontol. (2015). https://doi.org/10.1111/jcpe.12330.
17. G. Pini-Prato, D. Franceschi, F. Cairo, M. Nieri, R. Rotundo, Classification of Dental Surface Defects in Areas of Gingival Recession, J. Periodontol. 81 (2010) 885–890. https://doi.org/10.1902/jop.2010.090631.

18. B. Ibragimov, T. Vrtovec, Landmark-Based Statistical Shape Representations, 1st ed., Elsevier Ltd, 2017. https://doi.org/10.1016/B978-0-12-810493-4.00005-5.
19. H. Kim, E. Shim, J. Park, Y.J. Kim, U. Lee, Y. Kim, Web-based fully automated cephalometric analysis by deep learning, Comput. Methods Programs Biomed. 194 (2020). https://doi.org/10.1016/j.cmpb.2020.105513.
20. T. Joda, M.M. Bornstein, R.E. Jung, M. Ferrari, T. Waltimo, N.U. Zitzmann, Recent Trends and Future Direction of Dental Research in the Digital Era, Int. J. Environ. Res. Public Health. 17 (2020). https://doi.org/10.3390/ijerph17061987.
21. C.W. Wang, C.T. Huang, M.C. Hsieh, C.H. Li, S.W. Chang, W.C. Li, R. Vandaele, R. Marée, S. Jodogne, P. Geurts, C. Chen, G. Zheng, C. Chu, H. Mirzaalian, G. Hamarneh, T. Vrtovec, B. Ibragimov, Evaluation and Comparison of Anatomical Landmark Detection Methods for Cephalometric X-Ray Images: A Grand Challenge, IEEE Trans. Med. Imaging. (2015). https://doi.org/10.1109/TMI.2015.2412951.
22. C.W. Wang, C.T. Huang, J.H. Lee, C.H. Li, S.W. Chang, M.J. Siao, T.M. Lai, B. Ibragimov, T. Vrtovec, O. Ronneberger, P. Fischer, T.F. Cootes, C. Lindner, A benchmark for comparison of dental radiography analysis algorithms, Med. Image Anal. (2016). https://doi.org/10.1016/j.media.2016.02.004.
23. P.L. Lin, P.Y. Huang, P.W. Huang, Automatic methods for alveolar bone loss degree measurement in periodontitis periapical radiographs, Comput. Methods Programs Biomed. 148 (2017) 1–11. https://doi.org/10.1016/j.cmpb.2017.06.012.
24. F. Abdolali, R.A. Zoroofi, Y. Otake, Y. Sato, Automated classification of maxillofacial cysts in cone beam CT images using contourlet transformation and Spherical Harmonics, Comput. Methods Programs Biomed. 139 (2017) 197–207. https://doi.org/10.1016/j.cmpb.2016.10.024.
25. T. Vrtovec, B. Likar, F. Pernuš, Quantitative analysis of spinal curvature in 3D: Application to CT images of normal spine, Phys. Med. Biol. (2008). https://doi.org/10.1088/0031-9155/53/7/006.
26. A. Keeling, J. Wu, M. Ferrari, Confounding factors affecting the marginal quality of an intra-oral scan, J. Dent. 59 (2017) 33–40. https://doi.org/10.1016/j.jdent.2017.02.003.
27. C. Lippold, X. Liu, K. Wangdo, B. Drerup, K. Schreiber, C. Kirschneck, T. Moiseenko, G. Danesh, Facial landmark localization by curvature maps and profile analysis, Head Face Med. (2014). https://doi.org/10.1186/1746-160X-10-54.
28. L. Di Angelo, P. Di Stefano, S. Bernardi, M.A. Continenza, A new computational method for automatic dental measurement: The case of maxillary central incisor, Comput. Biol. Med. 70 (2016) 202–209. https://doi.org/10.1016/j.compbiomed.2016.01.018.
29. G. Farin, Curvature combs and curvature plots, CAD Comput. Aided Des. (2016). https://doi.org/10.1016/j.cad.2016.08.003.
30. J. Lindhe, T. Karring, M. Araújo, Anatomy of Periodontal Tissues, in: N.P. Lang, J. Lindhe (Eds.), Clin. Periodontol. Implant Dent., John Wiley & Sons Inc, New York, 2015: pp. 4–47.
31. P.M. Preshaw, L. Kupp, A.F. Hefti, A. Mariotti, Measurement of Clinical Attachment Levels using a constant-force periodontal probe modified to detect the Cemento-Enamel Junction, J. Clin. Periodontol. (1999). https://doi.org/10.1034/j.1600-051X.1999.260704.x.

32. M.K. Jeffcoat, R.L. Jeffcoat, S.C. Jens, K. Captain, A new periodontal probe with automated cemento-enamel junction detection, J. Clin. Periodontol. (1986). https://doi.org/10.1111/j.1600-051X.1986.tb02222.x.
33. K. Vandana, R. Haneet, Cementoenamel junction: An insight, J. Indian Soc. Periodontol. 18 (2014) 549–554. https://doi.org/10.4103/0972-124X.142437.
34. O. Zuhr, S.F. Rebele, K. Vach, H. Petsos, M.B. Hürzeler, Tunnel technique with connective tissue graft versus coronally advanced flap with enamel matrix derivate for root coverage: 2-year results of an RCT using 3D digital measuring for volumetric comparison of gingival dimensions., J. Clin. Periodontol. (2020). https://doi.org/10.1111/jcpe.13328.
35. J.W. Bartlett, C. Frost, Reliability, repeatability and reproducibility: Analysis of measurement errors in continuous variables, Ultrasound Obstet. Gynecol. 31 (2008) 466–475. https://doi.org/10.1002/uog.5256.
36. F. Cairo, G.P. Pini-Prato, A technique to identify and reconstruct the cementoenamel junction level using combined periodontal and restorative treatment of gingival recession. A prospective clinical study, Int. J. Periodontics Restor. Dent. 30 (2010) 573–581. https://doi.org/10.11607/prd.00.0945.
37. G. Zucchelli, G. Gori, M. Mele, M. Stefanini, C. Mazzotti, M. Marzadori, L. Montebugnoli, M. De Sanctis, Non-Carious Cervical Lesions Associated With Gingival Recessions: A Decision-Making Process, J. Periodontol. 82 (2011) 1713–1724. https://doi.org/10.1902/jop.2011.110080.
38. S.P. Bienz, I. Sailer, I. Sanz-Martín, R.E. Jung, C.H.F. Hämmerle, D.S. Thoma, Volumetric changes at pontic sites with or without soft tissue grafting: a controlled clinical study with a 10-year follow-up, J. Clin. Periodontol. 44 (2017) 178–184. https://doi.org/10.1111/jcpe.12651.
39. C. Fons-Badal, J. Alonso Pérez-Barquero, N. Martínez-Martínez, J. Faus-López, A. Fons-Font, R. Agustín-Panadero, A novel, fully digital approach to quantifying volume gain after soft tissue graft surgery. A pilot study, J. Clin. Periodontol. (2019) 0–2. https://doi.org/10.1111/jcpe.13235.
40. P. Parvini, M.E. Galarraga-Vinueza, K. Obreja, R. de S. Magini, R. Sader, F. Schwarz, Prospective study assessing three-dimensional changes of mucosal healing following soft tissue augmentation using free gingival grafts, J. Periodontol. 92 (2021) 400–408. https://doi.org/10.1002/JPER.19-0640.
41. M. Kuralt, R. Gašperšič, A. Fidler, 3D computer-aided treatment planning in periodontology: A novel approach for evaluation and visualization of soft tissue thickness, J. Esthet. Restor. Dent. 32 (2020) 457–462. https://doi.org/10.1111/jerd.12614.
42. D. Kloukos, G. Koukos, N. Gkantidis, A. Sculean, C. Katsaros, A. Stavropoulos, Transgingival probing: A clinical gold standard for assessing gingival thickness, Quintessence Int. (Berl). 52 (2021) 394–401. https://doi.org/10.3290/j.qi.b937015.
43. M.E. Galarraga-Vinueza, K. Obreja, R. Magini, A. Sculean, R. Sader, F. Schwarz, Volumetric assessment of tissue changes following combined surgical therapy of peri-implantitis: A pilot study, J. Clin. Periodontol. 47 (2020) 1159–1168. https://doi.org/10.1111/jcpe.13335.
44. D.S. Thoma, T.J.W. Gasser, R.E. Jung, C.H.F. Hämmerle, Randomized controlled clinical trial comparing implant sites augmented with a volume-stable collagen matrix or an autogenous

connective tissue graft: 3-year data after insertion of reconstructions, J. Clin. Periodontol. 47 (2020) 630–639. https://doi.org/10.1111/jcpe.13271.

45. M. Zeltner, R.E. Jung, C.H.F. Hämmerle, J. Hüsler, D.S. Thoma, Randomized controlled clinical study comparing a volume-stable collagen matrix to autogenous connective tissue grafts for soft tissue augmentation at implant sites: linear volumetric soft tissue changes up to 3 months, J. Clin. Periodontol. 44 (2017) 446–453. https://doi.org/10.1111/jcpe.12697.
46. M. Kuralt, A. Fidler, Assessment of reference areas for superimposition of serial 3D models of patients with advanced periodontitis for volumetric soft tissue evaluation, J. Clin. Periodontol. (2021). https://doi.org/10.1111/jcpe.13445.
47. J.S. Lee, Y.S. Jeon, F.J. Strauss, H.I. Jung, R. Gruber, Digital scanning is more accurate than using a periodontal probe to measure the keratinized tissue width, Sci. Rep. 10 (2020) 0–8. https://doi.org/10.1038/s41598-020-60291-0.

Figures

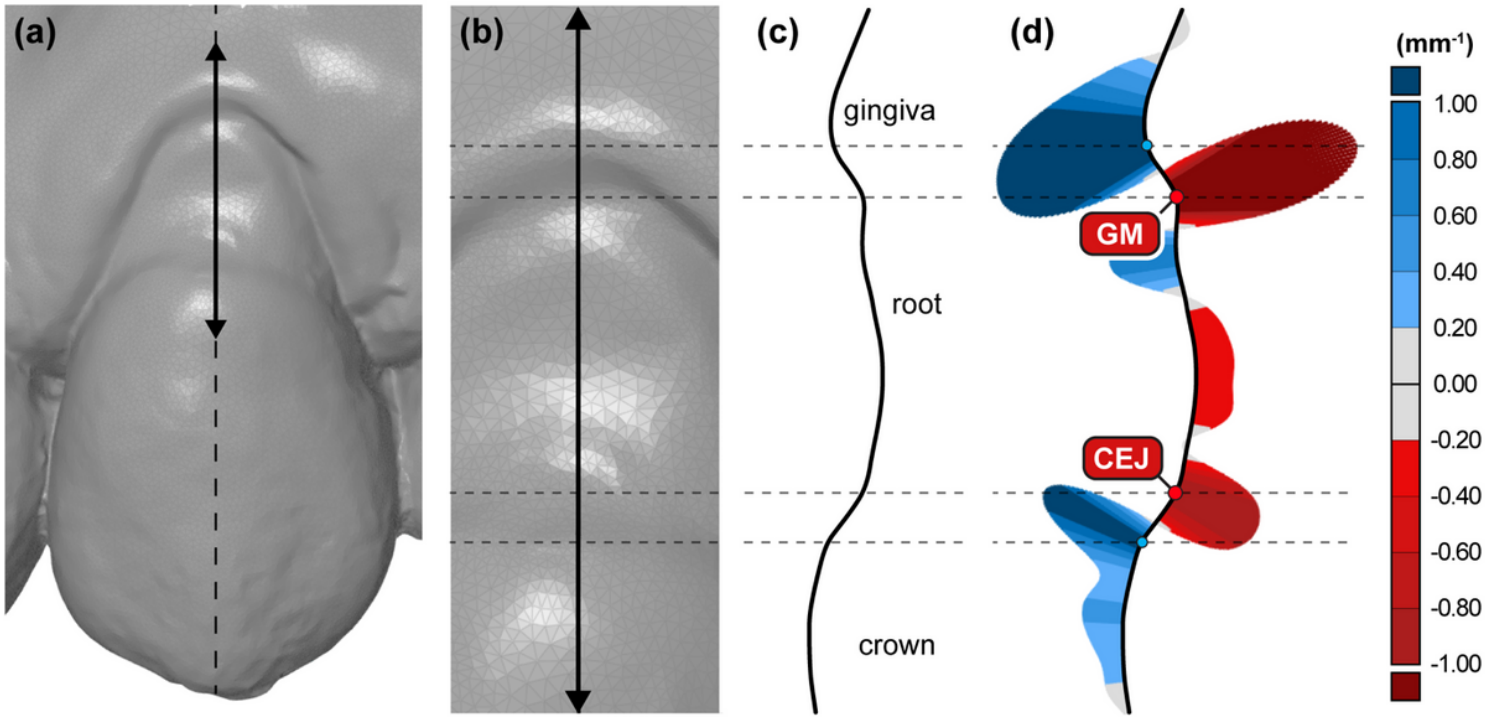

Figure 1

Automated measurement point selection by using curvature analysis on a representative cross-section. Digital model of maxillary left canine with a representative cross-section at the central buccal site in the direction of the long axis of the tooth (full black line) (a) and a corresponding close-up view (b). A side view of a cross-section (c) also depicting the view for manual measurement point selection. A "curvature comb", i.e., a graph that displays the curvature values at a specific point on an actual cross-section, is shown at (d). Two cross-section segments of interest are marked with dashed grey lines, defined with two

local extreme points with positive and negative curvature, i.e., maximum convexity (blue) and concavity (red), respectively. Both cemento-enamel junction (CEJ) and gingival margin (GM) points are defined as a local extreme point with maximum concavity (red) within the cross-section segments mentioned above.

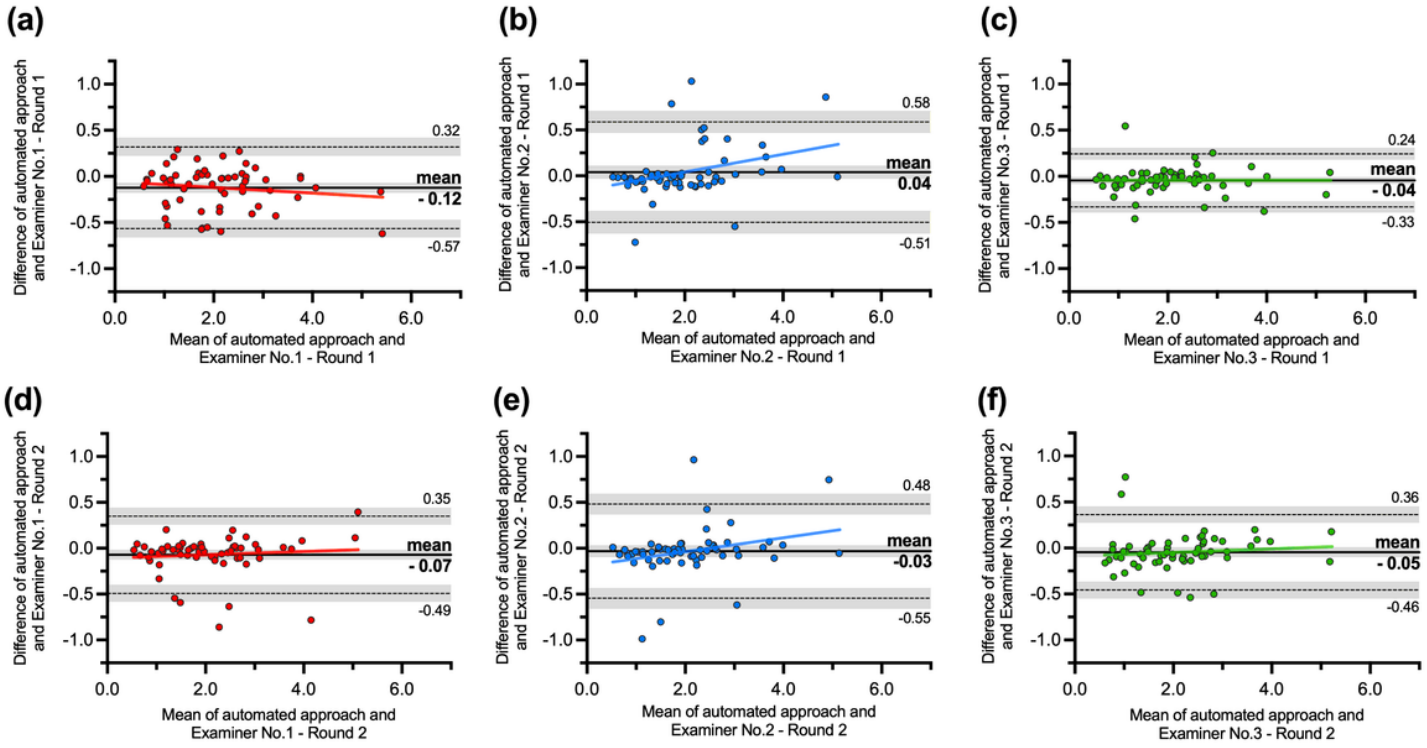

Figure 2

Bland-Altman plots showing a comparison of digital measurements of gingival recession between Examiner No. 1 (red dots), No. 2 (blue dots), and No. 3 (green dots) in the first (a-c) and second round of measurements (d-f) in reference to automated curvature-based approach. The x-axis indicates the mean measurement of the gingival recession between compared approaches. The y-axis indicates the difference between compared approaches. A black line with the surrounding grey area indicates mean bias and 95% confidence interval. A dashed black line with a surrounding grey area indicates either upper or lower 95% limits of agreement and corresponding 95% confidence interval.

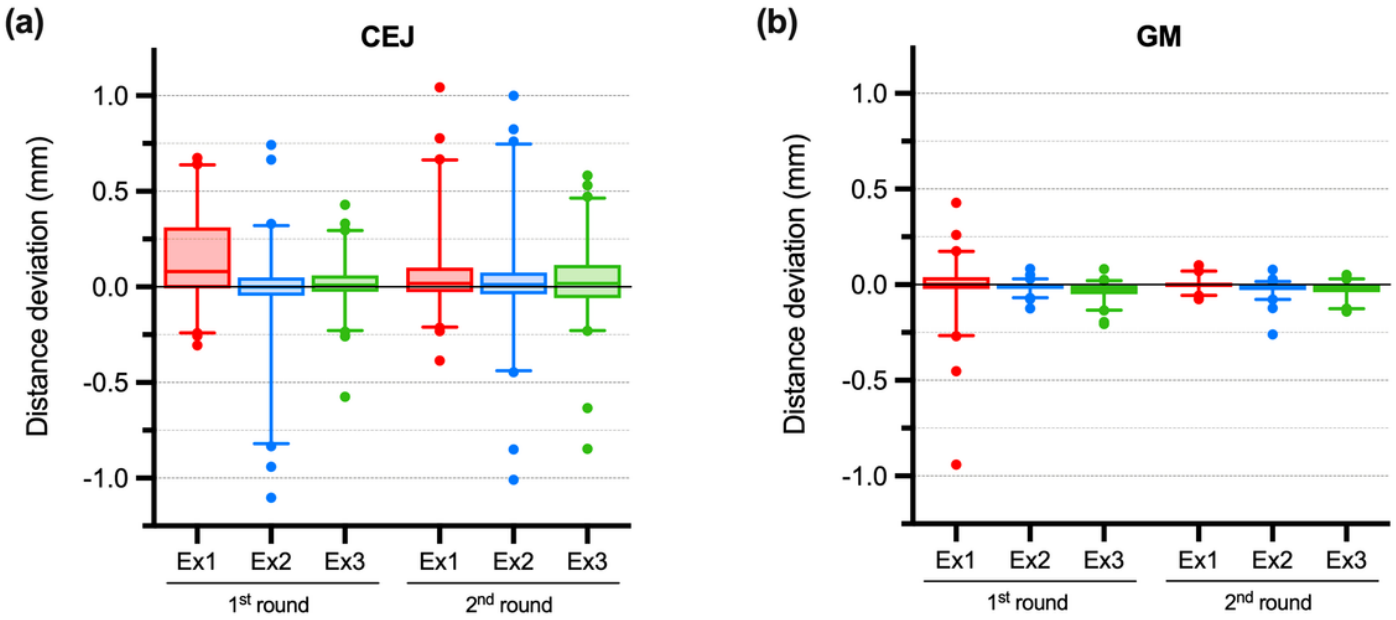

Figure 3

Manual measurement point selection variability depicted with box-plots with measurement point distance deviation of cemento-enamel junction (CEJ) (a) and gingival margin (GM) point (b) for each examiner and a round of measurement in reference to automated curvature-based point position on a cross-section. Box represent 25th and 75th percentile, while whisker represents 5th and 95th percentile and dots represent outliers.

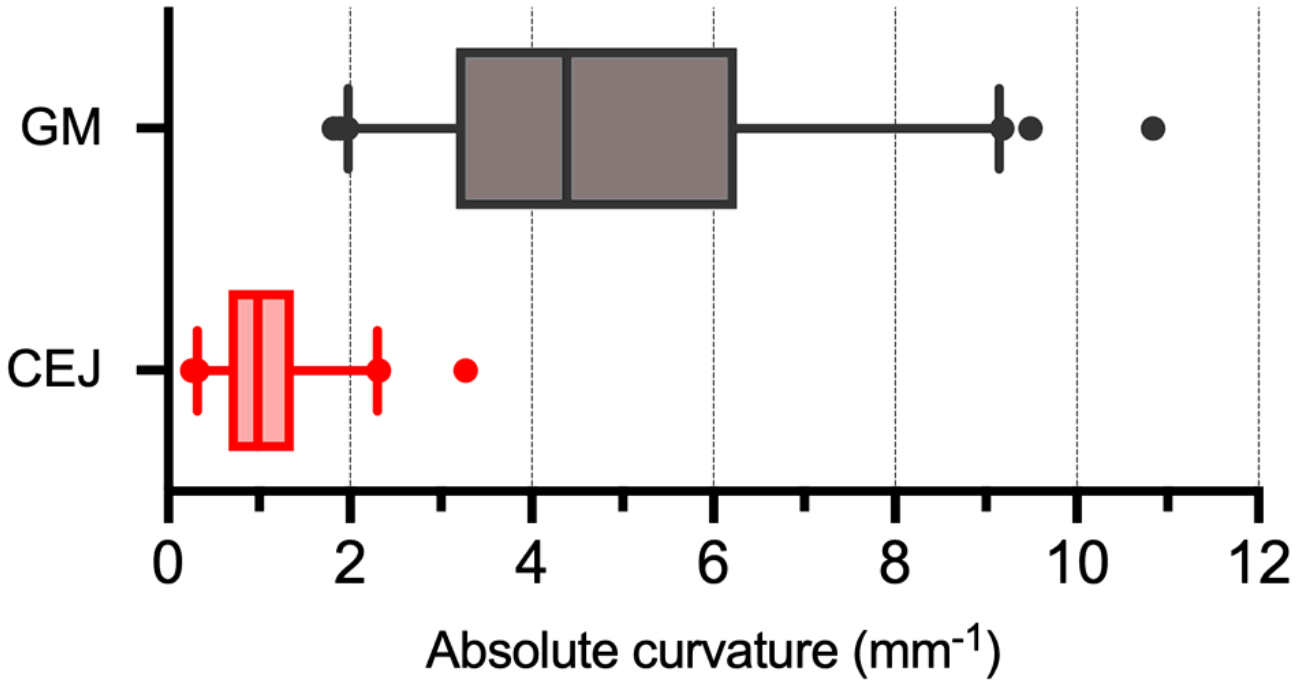

Figure 4

Profile shape description of cemento-enamel junction (CEJ) and gingival margin (GM) points using box-plots. Box represent the 25th and 75th percentile, while whiskers represent the 5th and 95th percentile, and dots represent outliers.

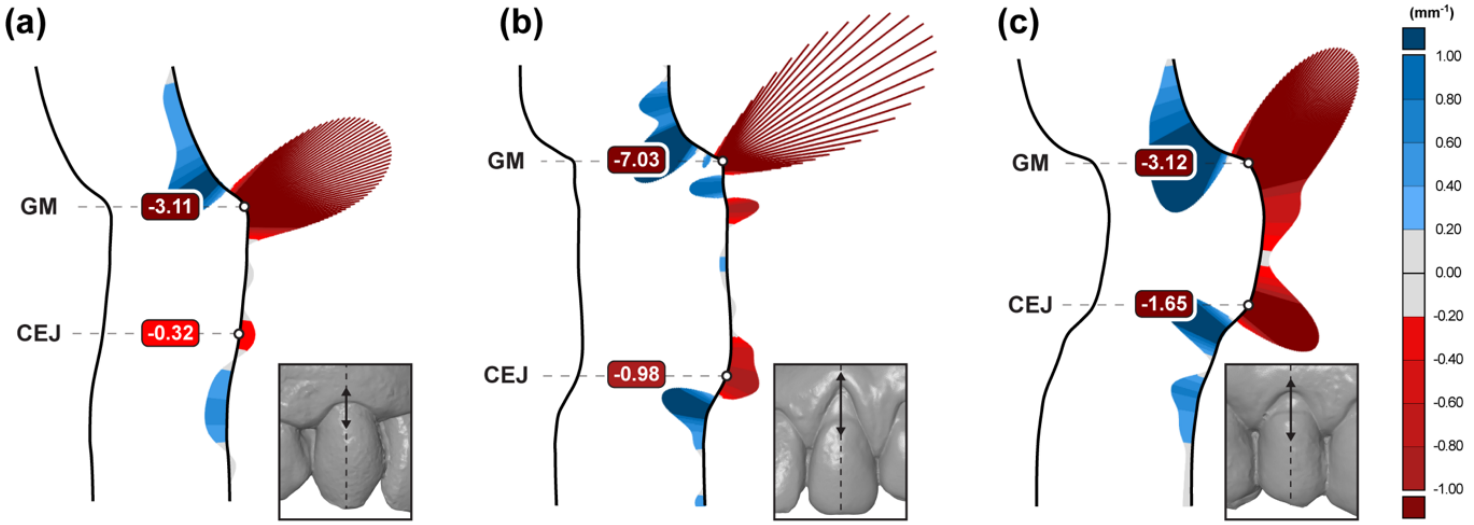

Figure 5

Cross-section shapes of representative gingival margin (GM) and cemento-enamel junction (CEJ) profiles with "curvature combs" graphs of three maxillary teeth, i.e., right canine (a), left canine (b), and right first premolar (c). Visual inspection of cross-section profiles and "curvature comb" graphs depicts GM point as more distinct and easier to select than CEJ point. Visually perceived shape differences at CEJ points compared to GM points are larger despite the smaller differences in curvature values, i.e., -0.32 mm-1 vs -0.98 mm-1 for CEJ points and -3.11 mm-1 vs -7.03 mm-1 for GM points (a and b, respectively). It results from the mathematical definition of curvature as a ratio, i.e., an inverse radius (1/r), and human perception, which more easily distinguish between the straight line and a circle than between two circles with a small difference in radius. Interestingly, similar GM curvature values in (a) and (c) produce different shapes of curvature comb graphs (figure (c) "curvature comb" in coronal direction), which can be explained as an effect of root surface defect present in (c).

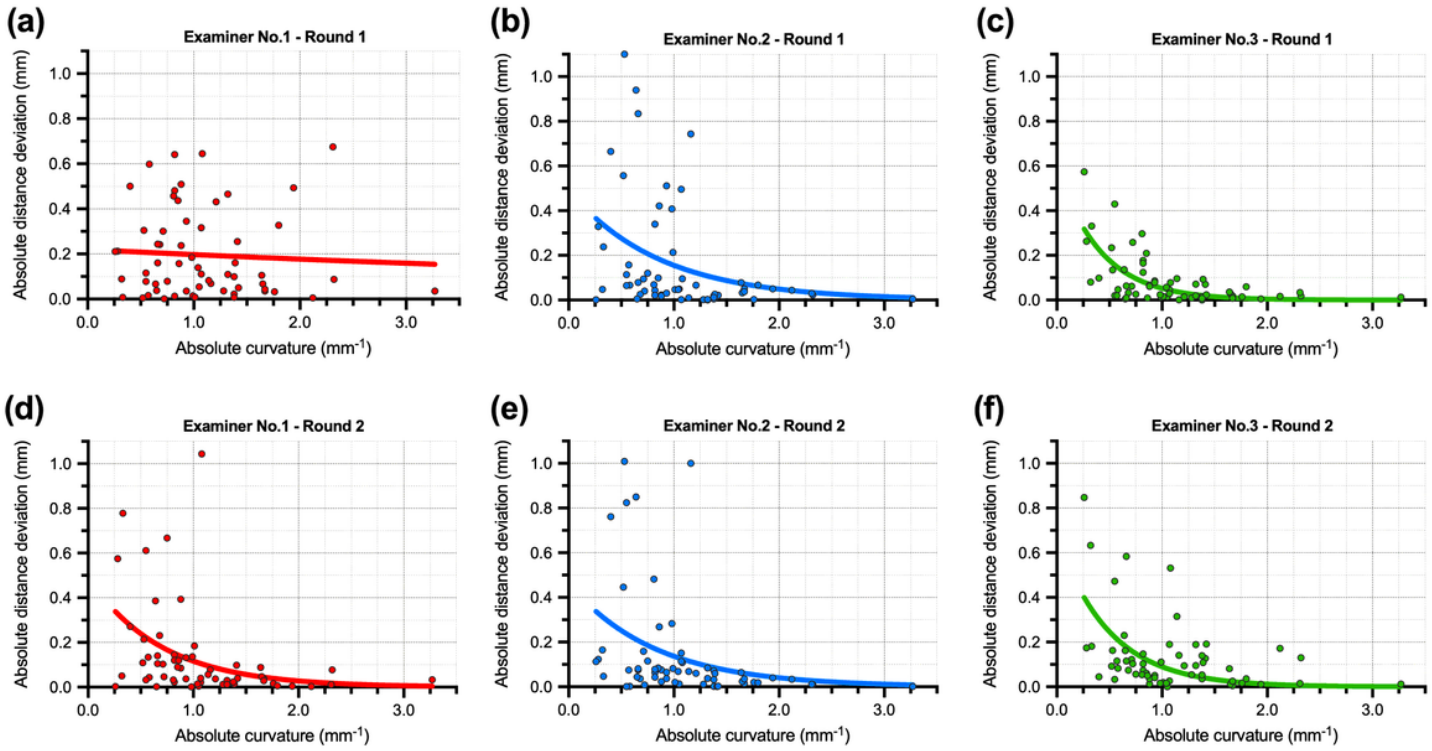

Figure 6

Scatter plots displaying correlation of curvature and manual CEJ points distance deviation, i.e., the distance between manual and automated curvature-based CEJ reference point position. The upper row shows the first round of measurement (a-c), and the lower row shows the second round of measurements (d-f). The same colour legend is used as in Figure 2 and 3, i.e., Examiner No. 1 - red, No. 2 - blue, and No. 3 – green.

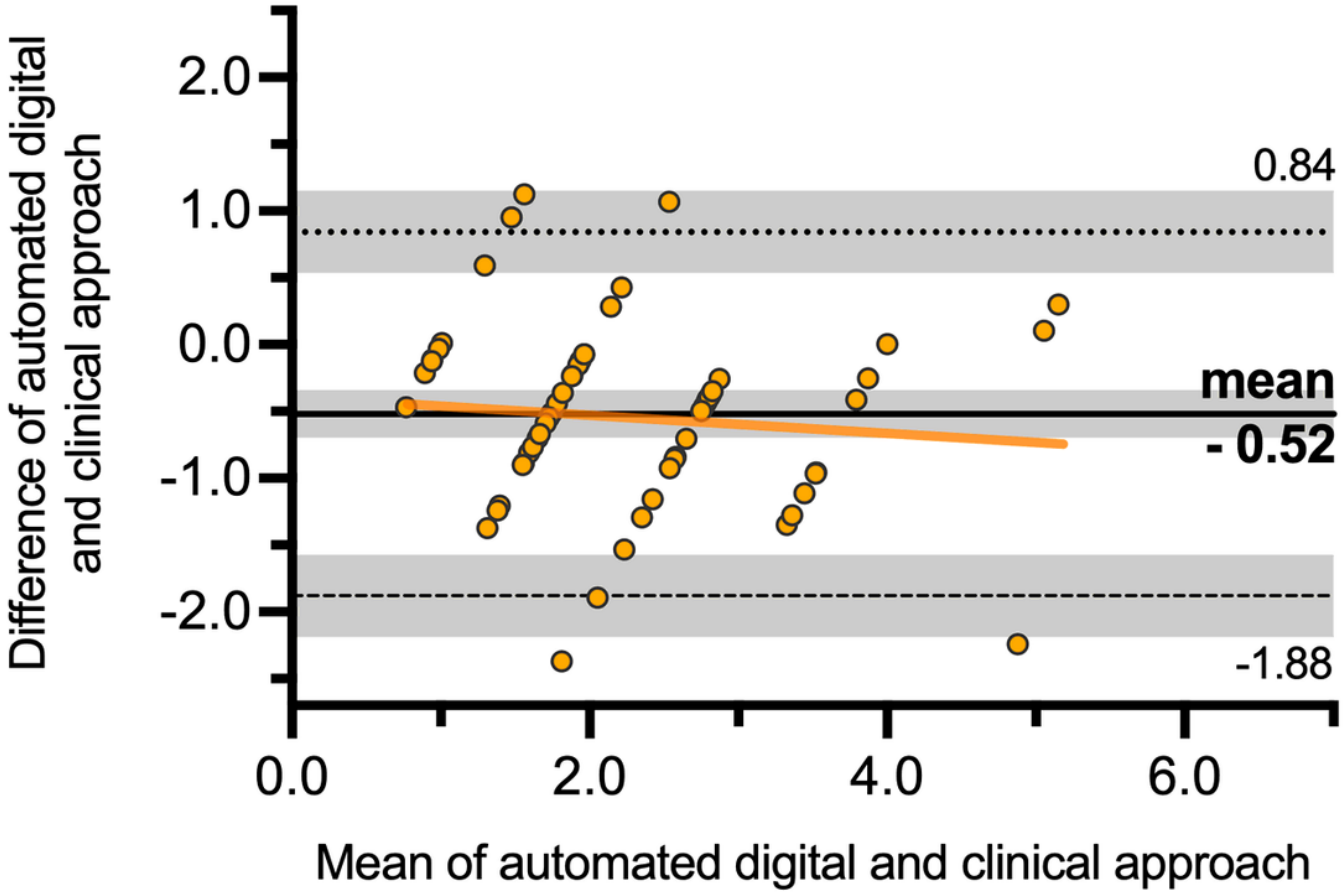

Figure 7

Bland-Altman plot showing a comparison of digital automated and clinical measurements of gingival recession in reference to automated curvature-based approach. The x-axis indicates the mean measurement of the gingival recession between compared approaches. The y-axis indicates the difference between compared approaches. A black line with the surrounding grey area indicates mean bias and 95% confidence interval. A dashed black line with a surrounding grey area indicates either upper or lower 95% limits of agreement and corresponding 95% confidence interval.